Biomolecular Feedback Systems

Domitilla Del Vecchio
U. Michigan/MIT

Richard M. Murray
Caltech

DRAFT v0.3, March 11, 2010

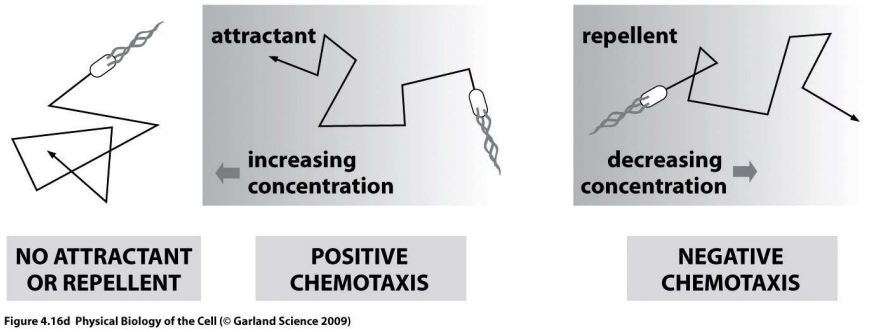

Figure 5.5: Examples of chemotaxis. Figure from Phillips, Kondev and Theriot [35]; used with permission of Garland Science.

5.4 Bacterial Chemotaxis

Chemotaxis refers to the process by which micro-organisms move in response to chemical stimuli. Examples of chemotaxis include the ability of organisms to move in the direction of nutrients or move away from toxins in the environment. Chemotaxis is called *positive chemotaxis* if the motion is in the direction of the stimulus and *negative chemotaxis* if the motion is away from the stimulant, as shown in Figure 5.5. Many chemotaxis mechanisms are stochastic in nature, with biased random motions causing the average behavior to be either positive, negative or neutral (in the absence of stimuli).

In this section we look in some detail at bacterial chemotaxis, which *E. coli* use to move in the direction of increasing nutrients. The material in this section is based primarily on the work of Barkai and Leibler [8] and Rao, Kirby and Arkin [37].

Control system overview

The chemotaxis system in *E. coli* consists of a sensing system that detects the presence of nutrients, and actuation system that propels the organism in its environment, and control circuitry that determines how the cell should move in the presence of chemicals that stimulate the sensing system. The approximate location of these elements are shown in Figure **??**.

The actuation system in the *E. coli* consists of a set of flagella that can be spun using a flagellar motor embedded in the outer membrane of the cell, as shown in Figure 5.6a. When the flagella all spin in the counter clockwise direction, the individual flagella form a bundle and cause the organism to move roughly in a straight line. This behavior is called a "run" motion. Alternatively, if the flagella spin in the clockwise direction, the individual flagella do not form a bundle and the organism "tumbles", causing it to rotate (Figure 5.6b). The selection of the motor direction is controlled by the protein CheY: if phosphorylated CheY binds to the

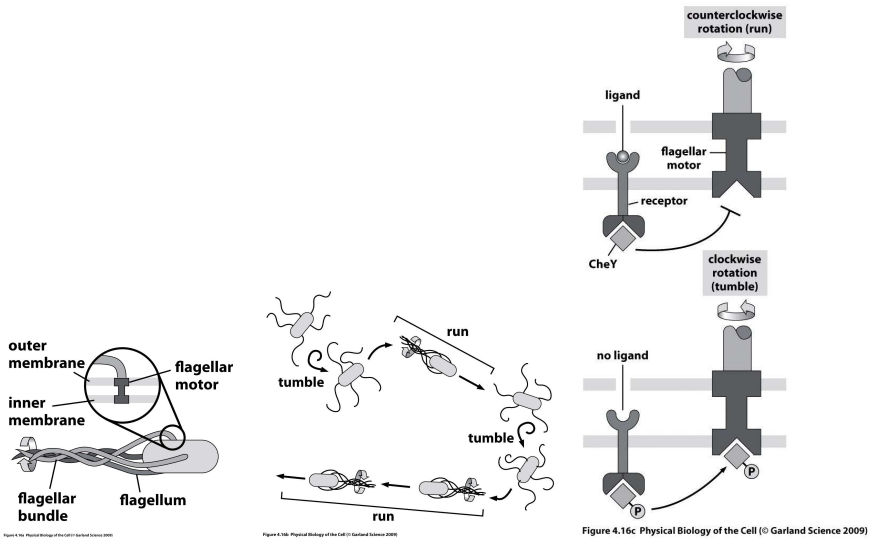

(a) (b) (c)

Figure 5.6: Bacterial chemotaxis. Figures from Phillips, Kondev and Theriot [35]; used with permission of Garland Science.

motor complex, the motor spins clockwise (tumble), otherwise it spins counter-clockwise (run).

Because of the size of the organism, it is not possible for a bacterium to sense gradients across its length. Hence, a more sophisticated strategy is used, in which the organism undergoes a combination of run and tumble motions. The basic idea is illustrated in Figure 5.6c: when high concentration of ligand (nutrient) is present, the CheY protein is left unphosphorylated and does not bind to the actuation complex, resulting in a counter-clockwise rotation of the flagellar motor (run). Conversely, if the ligand is present then the molecular machinery of the cell causes CheY to be phosphorylated and this modifies the flagellar motor dynamics so that a clockwise rotation occurs (tumble). The net effect of this combination of behaviors is that when the organism is traveling through regions of higher nutrient concentration, it continues to move in a straight line for a longer period before tumbling, causing it to move in directions of increasing nutrient concentration.

A simple model for the molecular control system that regulates chemotaxis is shown in Figure 5.7. We start with the basic sensing and and actuation mechanisms. A membrane bound protein MCP (methyl-accepting chemotaxis protein) that is capable of binding to the external ligand serves as a signal transducing element from the cell exterior to the cytoplasm. Two other proteins, CheW and CheA, form a complex with MCP. This complex can either be in an active or inactive state. In the active state, CheA is autophosphorylated and serves as a phosphotransferase

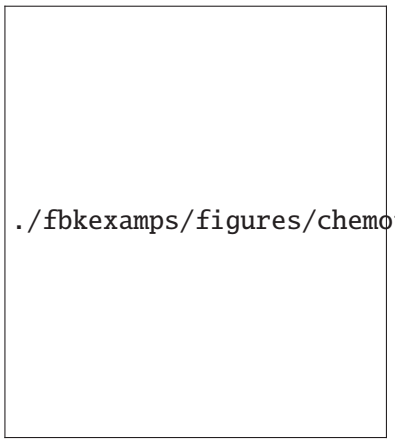

Figure 5.7: Control system for chemotaxis. Figure from Rao *et al*. [37] (Figure 1A).

for two additional proteins, CheB and CheY. The phosphorylated form of CheY then binds to the motor complex, causing clockwise rotation of the motor.

The activity of the receptor complex is governed by two primary factors: the binding of a ligand molecule to the MCP protein and the presence or absence of up to 4 methyl groups on the MCP protein. The specific dependence on each of these factors is somewhat complicated. Roughly speaking, when the ligand L is bound to the receptor then the complex is less likely to be active. Furthermore, as more methyl groups are present, the ligand binding probability increases, allowing the gain of the sensor to be adjusted through methylation. Finally, even in the absence of ligand the receptor complex can be active, with the probability increasing with increased methylation. Figure 5.8 summarizes the possible states, their free energies and the probability of activity.

Several other elements are contained in the chemotaxis control circuit. The most important of these are implemented by the proteins CheR and CheB, both of which affect the receptor complex. CheR, which is constitutively produced in the cell, methylates the receptor complex at one of the four different methylation sites. Conversely, the phosphorylated form of CheB demethylates the receptor complex. As described above, the methylation patterns of the receptor complex affect its activity, which affects the phosphorylation of CheA and, in turn, phosphorylation of CheY and CheB. The combination of CheA, CheB and the methylation of the receptor complex forms a negative feedback loop: if the receptor is active, then CheA phosphorylates CheB, which in turn demethylates the receptor complex, making it less active. As we shall see when we investigate the detailed dynamics below, this feedback loop corresponds to a type of integral feedback law. This integral action allows the cell to adjust to different levels of ligand concentration, so that the behavior of the system is invariant to the absolute nutrient levels.

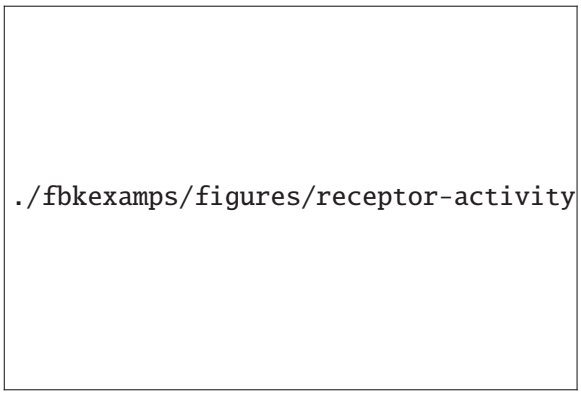

Figure 5.8: Receptor complex states. The probability of a given state being in an active configuration is given by p. Figure obtained from [30].

Modeling

The detailed reactions that implement chemotaxis are illustrated in Figure 5.9. Letting T represent the receptor complex and T^A represent an active form, the basic reactions can be written as

$$\begin{aligned} T^A + A &\rightleftharpoons T^A{:}A \longrightarrow A^p + T^A \\ A^p + B &\rightleftharpoons A^p{:}B \longrightarrow A + B^p \qquad B^p + P \rightleftharpoons B^p{:}P \longrightarrow B + P \\ A^p + Y &\rightleftharpoons A^p{:}Y \longrightarrow A + Y^p \qquad Y^p + Z \rightleftharpoons Y^p{:}Z \longrightarrow Y + Z \end{aligned} \tag{5.6}$$

where CheA, CheB, CheY and CheZ are written simply as A, B, Y and Z for simplicity and P is a non-specific phosphotase. We see that these are basically three linked sets of phosphorylation and dephosphorylation reactions, with CheA serving as a phosphotransferase and P and CheZ serving as phosphotases.

The description of the methylation of the receptor complex is a bit more complicated. Each receptor complex can have multiple methyl groups attached and the activity of the receptor complex depends on both the amount of methylation and whether a ligand is attached to the receptor site. Furthermore, the binding probabilities for the receptor also depend on the methylation pattern. To capture this, we use the set of reactions that are illustrated in Figures 5.7 and 5.9. In this diagram, T_i^s represents a receptor that has i methylation sites filled and ligand state s (which can be either u if unoccupied or o if occupied). We let M represent the maximum number of methylation sites ($M = 4$ for *E. coli*).

Using this notation, the transitions between the states correspond to the reactions shown in Figure 5.10:

$$\begin{aligned} T_i^x + B^p &\rightleftharpoons T_i^x{:}B^p \longrightarrow T_{i-1}^x + B^p && i > 0 \\ T_i^x + R &\rightleftharpoons T_i^x{:}R \longrightarrow T_{i+1}^x + R && i < M \\ T_i^u + L &\rightleftharpoons T_i^o \end{aligned}$$

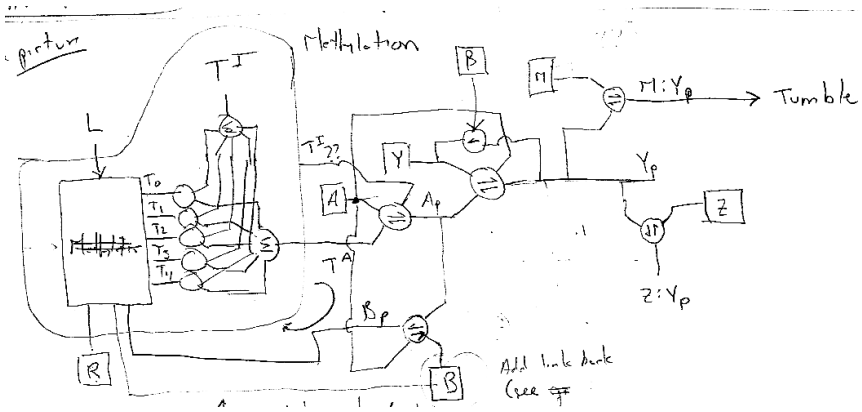

Figure 5.9: Circuit diagram for chemotaxis.

We now must write reactions for each of the receptor complexes with CheA. Each form of the receptor complex has a different activity level and so the most complete description is to write a separate reaction for each T_i^o and T_i^u species:

$$T_i^x + A \underset{k_i^{r,o}}{\overset{k_i^{f,o}}{\rightleftharpoons}} T_i^x{:}A \xrightarrow{k_i^{c,o}} A^p + T_i^x,$$

where $x \in \{o, u\}$ and $i = 0, \ldots, M$. This set of reactions replaces the placeholder reaction $T^A + A \rightleftharpoons T^A{:}A \longrightarrow A^p + T^A$ used earlier.

Approximate Model

The detailed model described above is sufficiently complicated that it can be difficult to analyze. In this section we develop a slightly simpler model that can be used to explore the adaptation properties of the circuit, which happen on a slower time-scale.

./fbkexamps/figures/chemotaxis-methylation.eps

Figure 5.10: Methylation model for chemotaxis. Figure from Barkai and Leibler [8] (Box 1). Note: the figure uses the notation E_i^s for the receptor complex instead of T_i^s.

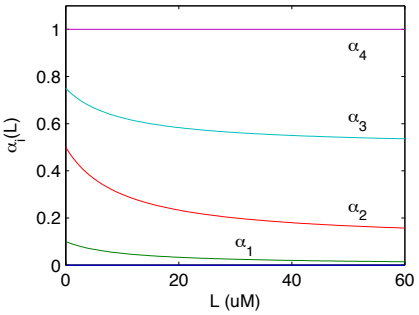

Figure 5.11: Probability of activity.

We begin by simplifying the representation of the receptor complex and its methylation pattern. Let $L(t)$ represent the ligand concentration and T_i represent the concentration of the receptor complex with i sides methylated. If we assume that the binding reaction of the ligand L to the complex is fast, we can write the probability that a receptor complex with i sites methylated is in its active state as a static function $\alpha_i(L)$, which we take to be of the form

$$\alpha_i(L) = \frac{\alpha_i^o L}{K_L + L} + \frac{\alpha_i K_L}{K_L + L}.$$

The coefficients α_i^o and α_i capture the effect of presence or absence of the ligand on the activity level of the complex. Note that α_i has the form of a Michaelis-Menten function, reflecting our assumption that ligand binding is fast compared to the rest of the dynamics in the model. Following [37], we take the coefficients to be

$$\begin{aligned} a_0 &= 0, & a_1 &= 0.1, & a_2 &= 0.5, & a_3 &= 0.75, & a_4 &= 1, \\ a_0^o &= 0, & a_1^o &= 0, & a_2^o &= 0.1, & a_3^o &= 0.5, & a_4^o &= 1. \end{aligned}$$

and choose $K_L = 10$ μM. Figure 5.11 shows how each α_i varies with L.

The total concentration of active receptors can now be written in terms of the receptor complex concentrations T_i and the activity probabilities $\alpha_i(L)$. We write the concentration of activated complex $\mathrm{T^A}$ and inactivated complex $\mathrm{T^I}$ as

$$T^A = \sum_{i=0}^{4} \alpha_i(L) T_i, \qquad T^I = \sum_{i=0}^{4} (1 - \alpha_i(L)) T_i.$$

These formulas can now be used in our dynamics as an effective concentration of active or inactive receptors, justifying the notation that we used in equation (5.6).

We next model the transition between the methylation patterns on the receptor. We assume that the rate of methylation depends on the activity of the receptor complex, with active receptors less likely to be demethylated and inactive receptors

less likely to be methylated [37, 30]. Let

$$r_B = k_B \frac{B^p}{K_B + T^A}, \qquad r_R = k_R \frac{R}{K_R + T^I},$$

represent rates of the methylation and demethylation reactions. We choose the coefficients as

$$k_B = 0.5, \quad K_B = 5.5, \quad k_R = 0.255, \quad K_R = 0.251,$$

We can now write the methylation dynamics as

$$\frac{d}{dt}T_i = r_R(1-\alpha_{i+1}(L))T_{i-1} + r_B\alpha_{i+1}(L)T_{i+1} - r_R(1-\alpha_i(L))T_i - r_B\alpha_i(L)T_i,$$

where the first and second terms represent transitions into this state via methylation or demethylation of neighboring states (see Figure 5.10) and the last two terms represent transitions out of the current state by methylation and demethylation, respectively. Note that the equations for T_0 and T_4 are slightly different since the demethylation and methylation reactions are not present, respectively.

Finally, we write the dynamics of the phosphorylation and dephosphorylation reactions, and the binding of $\mathrm{CheY^p}$ to the motor complex. Under the assumption that the concentrations of the phosphorylated proteins are small relative to the total protein concentrations, we can approximate the reaction dynamics as

$$\begin{aligned}
\frac{d}{dt}A^p &= 50T^A A - 100A^pY - 30A^pB,\\
\frac{d}{dt}Y^p &= 100A^pY - 0.1Y^p - 5[\mathrm{M}]Y^p + 19[\mathrm{M{:}Y^p}] - 30Y^p,\\
\frac{d}{dt}B^p &= 30A^pB - B^p,\\
\frac{d}{dt}[\mathrm{M{:}Y^p}] &= 5[\mathrm{M}]Y^p - 19[\mathrm{M{:}Y^p}].
\end{aligned}$$

The total concentrations of the species are given by

$$A + A^p = 5 \text{ nM}, \qquad B + B^p = 2 \text{ nM}, \qquad Y + Y^p + [\mathrm{M{:}Y^p}] = 17.9 \text{ nM},$$
$$[\mathrm{M}] + [\mathrm{M{:}Y^p}] = 5.8 \text{ nM}, \qquad R = 0.2 \text{ nM}, \qquad \textstyle\sum_{i=0}^{4} T_i = 5 \text{ nM}.$$

The reaction coefficients and concentrations are taken from Rao *et al*. [37].

Figure 5.12a shows a the concentration of the phosphorylated proteins based on a simulation of the model. Initially, all species are started in their unphosphorylated and demethylated states. At time $T = 500$ s the ligand concentration is increased to $L = 10$ μM and at time $T = 1000$ it is returned to zero. We see that immediately after the ligand is added, the $\mathrm{CheY^p}$ concentration drops, allowing longer runs between tumble motions. After a short period, however, the $\mathrm{CheY^p}$ concentration adapts to

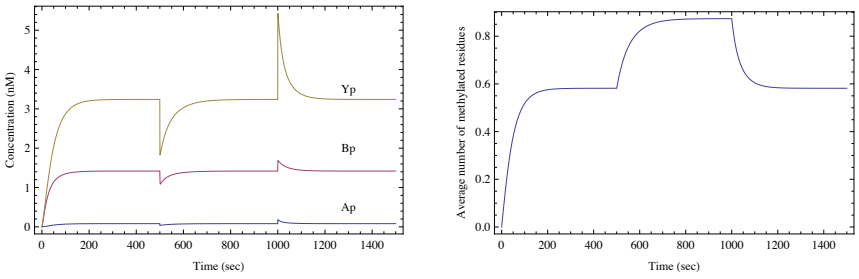

(a) (b)

Figure 5.12: Simulation and analysis of reduced-order chemotaxis model.

the higher concentration and the nominal run versus tumble behavior is restored. Similarly, after the ligand concentration is decreased the concentration of $\mathrm{CheY^p}$ increases, causing a larger fraction of tumbles (and subsequent changes in direction). Again, adaptation over a longer time scale returns that CheY concentration to its nominal value.

Figure 5.12b helps explain the adaptation response. We see that the average amount of methylation of the receptor proteins increases when the ligand concentration is high, which decreases the activity of CheA (and hence decreases the phosphorylation of CheY).

Integral action

The perfect adaptation mechanism in the chemotaxis control circuitry has the same function as the use of integral action in control system design: by including a feedback on the integral of the error, it is possible to provide exact cancellation to constant disturbances. In this section we demonstrate that a simplified version of the dynamics can indeed be regarded as integral action of an appropriate signal. This interpretation was first pointed out by Yi *et al* [48].

We begin by formulating an even simpler model for the system dynamics that captures the basic features required to understand the integral action. Let X represent the receptor complex and assume that it is either methylated or not. We let $\mathrm{X_m}$ represent the methylated state and we further assume that this methylated state can be activated, which we write as $\mathrm{X_m^*}$. This simplified description replaces the multiple states T_i and probabilities $\alpha_i(L)$. We also ignore the additional phosphorylation dynamics of CheY and simply take the activated receptor concentration X_m^* as our measure of overall activity.

Figure 5.13 shows the transitions between the various forms X. As before, CheR methylates the receptor and $\mathrm{CheB^p}$ demethylates it. We simplify the picture by only allowing $\mathrm{CheB^p}$ to act on the active state $\mathrm{X_m^*}$ and CheR to act on the inactive state. We take the ligand into account by assuming that the transition between the active

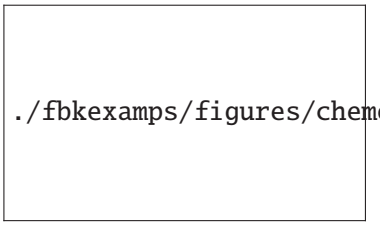

Figure 5.13: Reduced order model of receptor activity. Obtained from [3], Figure 7.9.

form X_m^* and the inactive form X_m depends on the ligand concentration: higher ligand concentration will increase the rate of transition to the inactive state.

This model is a considerable simplification from the ligand binding model that is illustrated in Figures 5.8 and 5.10. In the previous models, there is some probability of activity with or without methylation and with or without ligand. In this simplified model, we assume that only three states are of interest: demethylated, methylated/inactive and methylated/active. We also modify the way that that ligand binding is captured and instead of keeping track of all of the possibilities in Figure 5.8, we assume that the ligand transitions us from an active state X_m^* to an inactive X_m. These states and transitions are roughly consistent with the different energy levels and probabilities in Figure 5.8, but it is clearly a much coarser model.

Accepting these approximations, the model illustrated in Figure 5.13 results in a set of chemical reactions of the form

$$\begin{aligned}
&\mathrm{X} + \mathrm{R} \rightleftharpoons \mathrm{X{:}R} \longrightarrow \mathrm{X_m} + \mathrm{R} && \text{methylation} \\
&\mathrm{X_m^*} + \mathrm{B^p} \rightleftharpoons \mathrm{X_m^*{:}B^p} \longrightarrow \mathrm{X} + \mathrm{B^p} && \text{demethylation} \\
&\mathrm{X_m^*} \underset{k^r}{\overset{k^f(L)}{\rightleftharpoons}} \mathrm{X_m} && \text{activation/deactivation}
\end{aligned}$$

For simplicity we take both R and $\mathrm{B^p}$ to have constant concentration.

Approximating the first two reactions by their Michaelis-Menten forms and assuming that $X \gg 1$, we can write the resulting dynamics for the system as

$$\begin{aligned}
\frac{d}{dt} X_m &= k_R R + k^f(L) X_m^* - k^r X_m \\
\frac{d}{dt} X_m^* &= -k_B B^p \frac{X_m^*}{K_{X_m^*} + X_m^*} - k^f(L) X_m^* + k^r X_m.
\end{aligned}$$

We wish to use this model to understand how the steady state activity level X_m^* depends on the ligand concentration L (which enters through the deactivation rate $k^f(L)$). Starting with the first equation, we see that at equilibrium we have

$$X_{m,e} = (K_R/k^r)R.$$

To find $X^*_{m,e}$, we note that at equilibrium

$$0 = \frac{d}{dt}(X_{m,e} + X^*_{m,e}) = -k_B B^p \frac{X^*_{m,e}}{K_{X^*_m} + X^*_{m,e}} + k_R R.$$

From this equation we can solve for $X^*_{m,e}$ as a function of the CheR concentration:

$$X^*_{m,e} = \frac{K_{X^*_m} k_R R}{k_B B^p - k_R R}$$

Note that this solution does not depend on $k^f(L)$ or k^r and hence we see that the steady state solution is independent of the ligand concentration.

To see the integral action more directly, we write the dynamics in terms of a new variable $z = X^*_m - X^*_{m,e}$.

Further reading